



UNIVERSITY OF LEEDS

This is a repository copy of *Investigation of Ni/SiO<sub>2</sub> catalysts prepared at different conditions for hydrogen production from ethanol steam reforming*.

White Rose Research Online URL for this paper:  
<http://eprints.whiterose.ac.uk/115759/>

Version: Accepted Version

---

**Article:**

Wu, C, Dupont, V [orcid.org/0000-0002-3750-0266](https://orcid.org/0000-0002-3750-0266), Nahil, MA et al. (3 more authors) (2017) Investigation of Ni/SiO<sub>2</sub> catalysts prepared at different conditions for hydrogen production from ethanol steam reforming. *Journal of the Energy Institute*, 90 (2). pp. 276-284. ISSN 1743-9671

<https://doi.org/10.1016/j.joei.2016.01.002>

---

© 2016, Energy Institute. Published by Elsevier Ltd. Licensed under the Creative Commons Attribution-NonCommercial-NoDerivatives 4.0 International  
<http://creativecommons.org/licenses/by-nc-nd/4.0/>

**Reuse**

Unless indicated otherwise, fulltext items are protected by copyright with all rights reserved. The copyright exception in section 29 of the Copyright, Designs and Patents Act 1988 allows the making of a single copy solely for the purpose of non-commercial research or private study within the limits of fair dealing. The publisher or other rights-holder may allow further reproduction and re-use of this version - refer to the White Rose Research Online record for this item. Where records identify the publisher as the copyright holder, users can verify any specific terms of use on the publisher's website.

**Takedown**

If you consider content in White Rose Research Online to be in breach of UK law, please notify us by emailing [eprints@whiterose.ac.uk](mailto:eprints@whiterose.ac.uk) including the URL of the record and the reason for the withdrawal request.



[eprints@whiterose.ac.uk](mailto:eprints@whiterose.ac.uk)  
<https://eprints.whiterose.ac.uk/>

# Investigation of Ni/SiO<sub>2</sub> catalysts prepared at different conditions for hydrogen production from ethanol steam reforming

Chunfei Wu<sup>a,b\*</sup>, Valerie Dupont<sup>a</sup>, Mohamad Anas Nahil<sup>a</sup>,

Binlin Dou<sup>c</sup>, Haisheng Chen<sup>d</sup>, Paul T. Williams<sup>a\*</sup>

<sup>a</sup> Chemical & Process Engineering, University of Leeds, Leeds, LS2 9JT, UK

(Tel: +44 113 3432504; Email: p.t.williams@leeds.ac.uk)

<sup>b</sup> Department of Chemical Engineering, University of Hull, Hull, HU6 7RX, UK

(Tel: #44 1482466464; Email: c.wu@hull.ac.uk)

<sup>c</sup> School of Energy and Power Engineering, Dalian University of Technology 116023, Dalian, China

<sup>d</sup> Institute of Engineering Thermophysics, Chinese Academy of Sciences, Beijing, China

**Abstract:** Ni/SiO<sub>2</sub> catalysts prepared by a sol-gel method have been investigated for hydrogen production via steam reforming of ethanol using a continuous flow, fixed bed reactor system. Chemical equilibrium calculations were also performed to determine the effects of temperature and molar steam to carbon ratio on hydrogen production. The acidity of the preparation solution (modified by nitric acid and ammonia) and calcination atmosphere (air and N<sub>2</sub>) were investigated in the preparation of the catalysts. BET surface area and porosity, temperature-programmed oxidation (TPO), X-ray diffraction (XRD), transmission electron microscopy (TEM) and scanning electron microscopy (SEM) were used to characterise the prepared catalysts. The BET surface area was reduced when the solution acidity was lowered during the sol-gel preparation process. A pH value less than 2.0 was necessary to achieve high metal dispersion in the catalyst. Smaller NiO particles were obtained when the catalyst was calcined in N<sub>2</sub>. Material balances on ethanol steam reforming at 600 °C using the prepared Ni/SiO<sub>2</sub> catalysts were determined, and higher hydrogen production with lower coke deposition on the reacted catalysts were also obtained from the catalysts calcined in N<sub>2</sub> atmosphere.

Keywords: Sol-gel; Catalyst; Nickel; Hydrogen; Ethanol; Reforming

## 1. Introduction

Due to the environmental problems derived from utilization of fossil fuels and the consideration of energy security, more attention has been paid to the development of new energy fuels.<sup>1-3</sup> Hydrogen is regarded as one of the promising energy carriers due to its high energy mass density, waste-free combustion and the vast variety of raw materials that can be used for its production.<sup>4</sup> Among the oxygenated hydrocarbons used for hydrogen production, ethanol is highly advantageous as it is readily available, safe to transport and handle,<sup>5, 6</sup> and offers a high maximum theoretical yield of H<sub>2</sub> via steam reforming (26.3 wt% of the ethanol feed) compared to other renewable feedstocks (e.g. glycerol, acetic acid). For these reasons it has been extensively investigated in the steam reforming process.<sup>7-9</sup>

Catalysts play an important role in hydrogen production from ethanol steam reforming by improving the production of hydrogen and the efficiency of the energy balance.<sup>10, 11</sup> However, catalyst development remains an interesting topic for research due to the deactivation of the catalyst during the ethanol steam reforming process. Although some studies have revealed that noble metal-based catalysts performed well for ethanol steam reforming,<sup>12-14</sup> nickel based catalysts are one of the most attractive catalysts that have been investigated because of their effective catalytic activity and relatively low cost.<sup>15-17</sup>

The sol-gel catalyst preparation method has been shown to confer high surface area and pore volume as well as high Ni dispersion for nickel-based catalysts.<sup>18-20</sup> In addition, the physical and chemical properties of the produced catalyst have been significantly influenced by the preparation methods using, for example, different Ni contents,<sup>21</sup> solution acidity,<sup>22</sup> solution reagent (citric acid etc.),<sup>23</sup> and catalyst calcination atmosphere.<sup>24</sup> Ni/SiO<sub>2</sub> catalysts have been widely used in hydrogen production.<sup>25</sup> However, studies of the influence of

different preparation conditions using sol-gel methods for the preparation of Ni/SiO<sub>2</sub> catalysts and the influence on ethanol steam reforming are very limited.

In this paper, Ni/SiO<sub>2</sub> catalysts have been prepared under different acidities of the sol-gel solution, and the catalyst precursor was calcined under different atmospheres (air and N<sub>2</sub>). The physical and chemical properties of the catalysts were analysed and related to their performance in relation to hydrogen production from the steam reforming of ethanol. The objective of the paper was to provide information concerning the influence of preparation conditions of Ni/SiO<sub>2</sub> catalysts on hydrogen production from the catalytic steam reforming of ethanol.

## **2. Experimental**

### **2.1. Preparation of Ni/SiO<sub>2</sub> catalyst**

Ni/SiO<sub>2</sub> catalysts with a Ni content of 20 wt.% were prepared by a simple sol-gel method adapted from the literature.<sup>26</sup> Ni(NO<sub>3</sub>)<sub>2</sub>•6H<sub>2</sub>O (Sigma-Aldrich), anhydrous citric acid (Alfa Aesar), deionized water, absolute ethanol (Sigma-Aldrich) and tetraethyl silicate (TEOS) (Sigma-Aldrich) were used as raw materials. 0.01 mol of Ni(NO<sub>3</sub>)<sub>2</sub>•6H<sub>2</sub>O and 0.02 mol citric acid were first dissolved into 200 ml of absolute ethanol and stirred at 60 °C for 3 h. Then, 7 ml of deionized water and a given amount of nitric acid (HNO<sub>3</sub>/TEOS molar ratio of 0.04, 0.12 or 0.20) or given amount of ammonia solution (NH<sub>3</sub>OH/TEOS molar ratio of 0.04 or 0.20) were added into the solution. The pH value of the solution was recorded. The molar ratio of the TEOS/HNO<sub>3</sub> or TEOS/NH<sub>4</sub>OH was selected according to reported work,<sup>27,28</sup> and the isoelectric point of silica (pH value of 2.0). 8.7 ml of TEOS were then added to the solution. After drying at 80 °C in a water bath, the precursor was calcined at 450 °C in an air or N<sub>2</sub> atmosphere for 3 h. The prepared catalysts were assigned as Ni/SiO<sub>2</sub>-1 to Ni/SiO<sub>2</sub>-8,

respectively, with the preparation conditions reported in Table 1 (A-agent; B-agent/TEOS molar ratio; C-calcination atmosphere). All the catalysts used in this paper were crushed and sieved to granules with a size between 0.08 and 0.20 mm.

## 2.2. Characterization of catalysts

The BET (Brunauer, Emmett and Teller) surface area and the porosity of the prepared catalysts were determined using a NONA 2200e Surface Area and Pore Size Analyzer. Samples were initially degassed under vacuum for 3h before surface analysis. The system operates by measuring the quantity of nitrogen adsorbed onto or desorbed from a solid sample at different equilibrium vapour pressures.

The temperature-programmed oxidation (TPO) of the reacted catalysts was carried out using a Stanton-Redcroft thermogravimetric analyser (TGA and DTG) to determine the properties of the coked carbons deposited on the reacted catalysts. About 20 mg of the reacted catalyst was heated in air at  $15\text{ }^{\circ}\text{C min}^{-1}$  to a final temperature of  $800\text{ }^{\circ}\text{C}$ , with a dwell time of 10 minutes with air flow around  $50\text{ ml min}^{-1}$ .

Ni/SiO<sub>2</sub>-1, Ni/SiO<sub>2</sub>-4, Ni/SiO<sub>2</sub>-5 and Ni/SiO<sub>2</sub>-8 catalysts, i.e. representatives of the low/high pH and the Air/N<sub>2</sub> calcination atmosphere used in the preparation method, were analysed by X-ray diffraction (XRD). The analysis was carried out with a Philips PW 1050 Goniometer using a PW 1730 with a CuK $\alpha$  radiation X-ray tube. The sample was ground to less than  $75\text{ }\mu\text{m}$  size and loaded into the 20 mm aperture of an aluminium sample holder.

A high resolution scanning electron microscope (SEM, LEO 1530) was used to characterise and examine the fresh catalysts and the characteristics of the carbon deposited on the coked catalysts. Transmission electron microscopy (TEM) (FEI Tecnai TF20 FEG) coupled with an energy dispersive X-ray spectroscopy (EDXS) was used to determine the

fresh and reacted catalysts. For the TEM analysis, the samples were ground, dispersed with methanol, and then deposited on a Cu grid covered with a perforated carbon membrane.

### **2.3. Ethanol steam reforming with the Ni/SiO<sub>2</sub> catalysts**

The prepared Ni/SiO<sub>2</sub> catalysts were investigated for hydrogen production via steam reforming of ethanol using a bench scale fixed bed reaction system. A schematic diagram of the reaction system and experimental process have been presented in our previous work.<sup>29</sup>

During the experiment, a mixture of ethanol and deionized water was introduced into a pre-heated reactor section (190 °C) with a total flow rate of 3.44 g h<sup>-1</sup>, and was catalytically reformed in a second reactor section, where 0.8 g of the prepared Ni/SiO<sub>2</sub> catalyst (not pre-reduced) was placed. N<sub>2</sub> was used as a carrier gas during the experiments with a flow rate of 80 ml min<sup>-1</sup>. It should be noted that the catalyst would be expected to be initially auto-reduced during the reforming process, and as shown later, that the consumption of ethanol for catalyst reduction was negligible in this work. Chemical equilibrium of the ethanol/water/N<sub>2</sub> system was predicted at different molar steam to carbon ratios (S/C) up to 4, and for a range of temperatures up to 700 °C, using the code Chemical Equilibrium and Applications (CEA)<sup>30</sup> which relies on minimisation of Gibbs energy. As shown in Figure 1, and in agreement with Le Chatelier's principle, for a given temperature, hydrogen yield in wt.% of the ethanol feed increased significantly with the rise in S/C ratio from 0 to 3; however, only a slight incremental increase was obtained at a S/C of 4. We have shown in a previous study that as S/C approaches 6, the energy balance of ethanol steam reforming at atmospheric pressure equals that of thermal water splitting,<sup>31</sup> negating the benefits of using ethanol as a source of hydrogen. This is caused by the energy burden of raising excess steam. It then becomes inefficient to carry out ethanol steam reforming at a S/C larger than 4 at atmospheric pressure.

Figure 1 also shows that the equilibrium hydrogen yield was maximized at the reforming temperature of 600 °C with the S/C of 4. For temperatures above 600 °C, reverse water gas shift was favoured, thus reducing the overall H<sub>2</sub> yield. Based on these chemical equilibrium calculations, the S/C ratio of 4 and reforming temperature of 600 °C were used to evaluate experimentally the performance of the catalysts in this work.

Condensable products were collected by using an air cooled condenser and a dry ice cooled condenser. The non-condensed gases, derived from around 1.5 hour reaction time, were collected with a Tedlar<sup>TM</sup> gas sample bag and analyzed for their components concentration by gas chromatography (GC). The conditions of GC and the gas analysis process have been described in our previous report.<sup>29</sup> Gas yield, calculated from the mass of gaseous products divided by the mass of the injected sample, and liquid yield, determined from the mass of condensed products divided by the mass of the injected sample, are presented in this work. Experiments were repeated to ensure the reliability of the results.

### **3. Results and discussion**

#### **3.1. Characterization of the Ni/SiO<sub>2</sub> catalysts**

##### **3.1.1. XRD analysis**

Crystal phases in the prepared Ni/SiO<sub>2</sub> catalysts were identified using XRD analysis. As shown in Figure 2, an amorphous peak at around 23 °, assigned to SiO<sub>2</sub>, was obtained for all the catalysts. Only a crystalline NiO phase was observed for the catalysts calcined in air, while a crystalline Ni phase was observed in the catalyst calcined in N<sub>2</sub> (Figure 2). Similar XRD patterns for Ni/SiO<sub>2</sub> catalyst calcined in air have been reported in other work.<sup>32, 33</sup> The Ni crystal phase was also found in the catalyst calcined in N<sub>2</sub>.<sup>24</sup>

### 3.1.2. Surface analysis

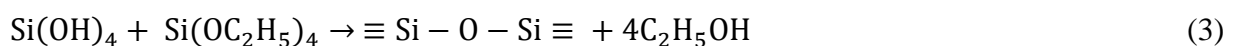
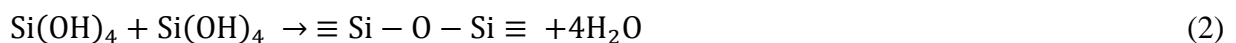
Surface properties of the prepared Ni/SiO<sub>2</sub> catalysts are shown in Table 1. BET surface area was reduced from 829 to 605 m<sup>2</sup> g<sup>-1</sup> for the catalyst calcined in air when the solution acidity was reduced, corresponding to an increase of pH value from 1 to 2; however, there was no obvious relationship between the solution acidity and the BJH pore volume. Small changes were observed for the BET surface area for the catalysts calcined in N<sub>2</sub>; however, the lowest BET surface area (545 m<sup>2</sup> g<sup>-1</sup>) was obtained for the Ni/SiO<sub>2</sub>-8 catalyst which was prepared under the most basic sol-gel solution (Table 1). Results of BJH pore diameter indicate that about 3.8 nm pore diameter was obtained for all the prepared catalysts except those produced under a NH<sub>4</sub>OH/TEOS molar ratio of 0.2.

The pore size distribution (Figure 3 and Figure 4) shows that the Ni/SiO<sub>2</sub>-4 and Ni/SiO<sub>2</sub>-8 catalysts prepared with the lowest acidity had a smaller fraction of pores at ~3.8 nm, compared with catalysts prepared under other acidities. The N<sub>2</sub> absorption/desorption isotherms of the selected catalysts are shown in Figure 3, which suggest that the catalysts show a combination of type I and IV (IUPAC classification) indicating a meso-porous structure in the catalysts.<sup>34</sup> Compared with catalysts calcined in N<sub>2</sub>, the Ni/SiO<sub>2</sub>-1 and Ni/SiO<sub>2</sub>-4 prepared in air showed higher N<sub>2</sub> absorption when the P/P<sub>0</sub> ratio was higher than 0.5. It is suggested that the catalysts prepared in air had more meso-pores compared with the catalysts prepared in N<sub>2</sub>. In terms of the pH of the preparation solution, a lower pH value seemed to produce a catalyst with more meso- and larger pores. For example, the Ni/SiO<sub>2</sub>-1 catalyst (pH=1.0) exhibited much higher N<sub>2</sub> absorption when the P/P<sub>0</sub> ratio was higher than 0.5, compared with the Ni/SiO<sub>2</sub>-4 catalyst (pH=2.08) (Figure 3). Therefore, from Table 1 and Figure 3, it is suggested that total surface area and pore volume are slightly changed, when the pH value of the catalyst preparation solution was lower than 2.0. However, both pore size

and surface area are significantly reduced resulting from the reduction of pore size, when the pH value of catalyst preparation solution was above 2.0.

### 3.1.3. TEM analysis

Transmission electron microscope analysis was carried out on the fresh calcined catalysts, and the results are shown in Figure 4. Smaller particle sizes were obtained for the catalysts prepared in N<sub>2</sub> compared to those prepared in air. In addition, similar particle dispersion was obtained for the catalysts calcined under air and nitrogen atmosphere, respectively, except those prepared at a NH<sub>4</sub>OH/TEOS molar ratio of 0.20. Unexpectedly large particles were observed for the Ni/SiO<sub>2</sub>-4 and Ni/SiO<sub>2</sub>-8 catalysts (Figure 4). It should be noted that precipitation occurred when the ammonia solution (NH<sub>4</sub>OH/TEOS molar ratio of 0.20) was added to the solution during the sol-gel preparation process; and this was observed before adding the TEOS to the solution. The large particles in the Ni/SiO<sub>2</sub>-4 and Ni/SiO<sub>2</sub>-8 catalysts were determined to be SiO<sub>2</sub> through EDXS analysis. The observation of large SiO<sub>2</sub> particles with the Ni/SiO<sub>2</sub>-4 and Ni/SiO<sub>2</sub>-8 catalysts is also consistent with the surface analysis, where these two catalysts exhibited obvious lower porosity compared to the other catalysts. It can be suggested that condensation was dominant (Reaction (2) and (3)) during the preparation of Ni/SiO<sub>2</sub>-4 and Ni/SiO<sub>2</sub>-8 catalysts where the co-precipitated solution was more basic,<sup>24</sup> resulting in the production of large SiO<sub>2</sub> particles. Therefore, in this work, a pH value of the preparation solution of less than 2.0 is suggested in order to obtain a high NiO dispersion.



## 3.2. Ethanol steam reforming using the Ni/SiO<sub>2</sub> catalyst

### 3.2.1. Mass balance and hydrogen production

As seen previously in Figure 1, hydrogen yield, expressed as weight percent of ethanol feed is expected, from equilibrium calculations, to increase with the increase of temperature to 600 °C as well as with S/C, and then declines slightly above 600 °C due to reverse water gas shift.

The experimental hydrogen production and mass balance during ethanol steam reforming with the eight prepared Ni/SiO<sub>2</sub> catalysts at 600 °C and S/C of 4 are shown in Table 2. Results in Table 2 reveal notable differences between the catalysts calcined in air and in N<sub>2</sub>. Measured gas yields were higher for the catalysts calcined in N<sub>2</sub>, with a yield around 64 wt.% of the total feed (ethanol+water), compared to a gas yield around 57 wt.% for the catalysts calcined in air. Measured liquid products show a slight difference. Measured carbon deposits on the catalyst calculated from the weight loss profiles under TPO were about 0.15 wt.% of feed. Overall the products balance closure was significantly better for the N<sub>2</sub> than for the air- calcined catalysts (2.5 wt.% vs. 6.4 wt.%). It is estimated that the balance closure value (sum of the measured product yields as a difference to 100 wt.%) was caused by carbon rich deposits (e.g tars) forming on the reactor which could not subsequently be recovered, as well as by experimental errors. It is likely that the larger this value, the more significant were the un-measured carbon rich deposits.

Finally, the measured H<sub>2</sub> yield expressed in percent of the equilibrium value of 23.2 wt.% of EtOH was higher for the N<sub>2</sub> than for the air calcined catalysts, averaging 71 wt.% vs. 67 wt.%. These values also indicated the reactor conditions were some distance from equilibrium, which allowed for better comparison between catalyst's activities. A calculation was performed to assess whether initial auto-reduction of the catalysts calcined in air as per reaction (5), which would have used the ethanol feed without net H<sub>2</sub> production, could have

accounted for the measured difference in H<sub>2</sub> yields between the air-calcined and the N<sub>2</sub>-calcined catalysts.



For 0.8 g of catalyst with 20 wt.% Ni loading, 2.726 mmol of NiO would have required reduction, representing an ethanol consumption of 1.7 wt.% of the ethanol feed over 1.5 h of experiment. Correcting the H<sub>2</sub> yield in wt.% of ethanol feed when the latter was diminished by 1.7 wt.% only increased the H<sub>2</sub> yield by 1 wt.%, whereas the average gap between H<sub>2</sub> yields by air-calcined (uncorrected for autoreduction) and N<sub>2</sub>-calcined catalysts was of 4 wt.%. This indicated that the benefits in H<sub>2</sub> yield of performing catalyst calcination in a nitrogen atmosphere rather than air on the H<sub>2</sub> yield were genuine. Clearly significant additional benefits were shown in the improved balance closure, lower coking on the catalyst, and higher gas yield to the detriment of the liquid yield, which includes unconverted ethanol and water.

When examining more closely which of the N<sub>2</sub>-calcined catalysts performed the most effectively, catalyst Ni/SiO<sub>2</sub>-7 provided the highest H<sub>2</sub> yield and purity due to a combination of lower carbon-products selectivity to methane and to CO (Table 3). Methane and CO by-product represent a penalty in H<sub>2</sub> yield and purity due to lack of conversion by steam methane reforming and by water gas shift respectively, therefore low selectivity in both CH<sub>4</sub> and CO is desirable. Table 3 shows the selectivity to the carbon and hydrogen containing products for all the catalysts, compared to the calculated equilibrium values. These show that selectivity to CH<sub>4</sub> in all the experiments was significantly higher and selectivity to CO<sub>2</sub> lower than the equilibrium value for both calcination atmospheres (~11 % for air-calcined catalysts, ~12 % for N<sub>2</sub>-calcined catalysts, compared to ~2 % at equilibrium), consistent with a kinetically favoured exothermic methanation to the detriment of the endothermic steam methane reforming.

The more effective performance of the catalysts for hydrogen production prepared under N<sub>2</sub> calcination is ascribed to the higher Ni metal dispersion in the catalyst. From XRD analysis (Figure 2), Ni diffraction peaks are barely observed for the catalysts calcined under N<sub>2</sub>, indicating fine Ni particles are presented. In contrast, sharp diffraction could be clearly observed for the catalysts calcined under air atmosphere, indicating the presence of large NiO particles. Additionally, a particle size of around 20 nm can be clearly observed from TEM analysis for the Ni/SiO<sub>2</sub> (1-3) catalysts calcined under air, while much smaller particles of around 4 nm could be found for the Ni/SiO<sub>2</sub> (5-7) catalysts calcined in N<sub>2</sub>.

Although calcination atmosphere has shown significant influence on hydrogen production from ethanol steam reforming, little changes in gas yield could be observed for the catalysts prepared under different acidities (Table 2). This phenomenon might be due to the similarities of surface properties and chemical properties of the catalysts (similar level of surface area and metal particle size) prepared at different acidity conditions calcined under the same atmosphere (Table 1). In addition, although some large particles could be observed for the Ni/SiO<sub>2</sub>-4 and Ni/SiO<sub>2</sub>-8 catalysts, the majority of small metal particles, similar to other catalysts, could also be observed from the TEM analysis (Figure 4), for the catalysts calcined under N<sub>2</sub> and air, respectively.

### **3.2.2. Coke formation on the reacted catalysts**

Coke deposition is one of the major challenges for catalyst development during ethanol steam reforming. In this section, the reacted catalysts were characterised by TPO experiments and SEM and TEM analysis for discussion of coke formation. TPO-TGA and TPO-DTG results are shown in Figure 5. The increasing mass peak in the TPO-TGA thermogram is assigned to oxidation of Ni particles which were reduced from the NiO phases by the reducing gases such

as ethanol, its reaction intermediates, H<sub>2</sub> and CO during ethanol steam reforming. Previous work<sup>31</sup> showed how ethanol alone and an ethanol/ bio-oil mixture could successfully autoreduce NiO catalysts at 600 °C and a S/C of 3.3. From Figure 5, one oxidation peak in the TPO-DTG analysis was obtained due to combustion of deposited carbons, which were assigned to filamentous carbons. In addition, the filamentous carbons were confirmed from the SEM and TEM results (Figure 6).

Coke deposition after ethanol steam reforming for each reacted catalyst is presented in Table 2. It is noted that the possible overlapping between Ni and coke oxidation was neglected during the TPO experiment. The amount of coke deposition was obtained from the TPO analysis; calculated as the mass difference between the sample weight (after water evaporation) and the mass of residue divided by the sample weight (after water evaporation). Low coke deposition was found on the Ni/SiO<sub>2</sub> catalysts, however, the reaction time used in this work of 1.5 h was short in relation to industrial scale processes. Longer reaction times, catalyst deactivation studies and catalyst recycling studies are recommended for future work to determine the effectiveness of the catalysts in relation to coking characteristics. From Figure 5 and Table 2, more carbon deposition was observed on the reacted catalyst calcined in air. It is suggested that smaller Ni particle size benefits the prohibition of coke formation on the surface of the catalyst. Kong et al.<sup>35</sup> investigated toluene reforming by various nickel catalysts, and reported that a larger amount of coke deposition was obtained for the catalyst (Ni/ZrO<sub>2</sub> and Ni/SiO<sub>2</sub>) with large Ni particle size (23.6, and 26.8 nm, respectively) compared with the Ni/Al<sub>2</sub>O<sub>3</sub> and Ni/MgO catalysts with Ni particle sizes less than 10 nm. Small Ni particle size was also reported to prohibit coke formation on a Ni-based catalyst during steam methane reforming.<sup>36</sup>

## Conclusions

The results show that the catalyst prepared using the sol-gel method has high surface area ( $>700 \text{ m}^2 \text{ g}^{-1}$ ) and narrow pore size distribution (pore diameter is around 3.8 nm), except for the catalyst prepared at a TEOS/ $\text{NH}_3\text{OH}$  ratio of 1:0.20. When the catalysts (Ni/SiO<sub>2</sub>-4 and Ni/SiO<sub>2</sub>-8 catalysts) were prepared with the lowest solution acidity, large SiO<sub>2</sub> particles and the lowest porosity were obtained. However, the solution acidity showed little influence on the gas yield and hydrogen concentration.

Ni and NiO crystal phases were identified by XRD analysis in the catalyst calcined in N<sub>2</sub>, however, only one NiO phase was identified in the catalyst calcined in air. Catalysts prepared in N<sub>2</sub> showed a higher Ni dispersion and resulted in higher gas yield with higher hydrogen production during ethanol steam reforming, compared with those calcined in air. The coke formation on the catalyst increased with the increase of basicity of the preparation solution for the Ni/SiO<sub>2</sub> catalyst.

### **Acknowledgements**

This work was supported by the International Exchange Scheme from the Royal Society (IE121244).

## References

- [1] Y. Himri, A.S. Malik, A. Boudghene Stambouli, S. Himri, and B. Draoui, Review and use of the Algerian renewable energy for sustainable development. *Renew. Sust. Energy Rev.* 2009, **13**, 1584-1591.
- [2] S.H. Jensen, P.H. Larsen, and M. Mogensen, Hydrogen and synthetic fuel production from renewable energy sources. *Int. J. Hydrogen Energy* 2007, **32**, 3253-3257.
- [3] F. Marias, S. Letellier, P. Cezac, and J.P. Serin, Energetic analysis of gasification of aqueous biomass in supercritical water. *Biomass Bioenerg.* 2011, **35**, 59-73.
- [4] C. Wu, and P.T. Williams, Hydrogen production by steam gasification of polypropylene with various nickel catalysts. *Appl. Catal. B: Environ.* 2009, **87**, 152-161.
- [5] M. Murdoch, G.I.N. Waterhouse, M.A. Nadeem, J.B. Metson, M.A. Keane, R.F. Howe, J. Llorca and H. Idriss, The effect of gold loading and particle size on photocatalytic hydrogen production from ethanol over Au/TiO<sub>2</sub> nanoparticles. *Nat. Chem.* 2011, **3**, 489-492.
- [6] R. Espinal, A. Anzola, E. Adrover, M. Roig, R. Chimentao, F. Medina, E. López, D. Borio, and J. Llorca, Durable ethanol steam reforming in a catalytic membrane reactor at moderate temperature over cobalt hydroxalcalite. *Int. J. Hydrogen Energy*, 2014, **39**, 10902-10910.
- [7] W. Cai, F. Wang, A. van Veen, C. Descorme, Y. Schuurman, W. Shen, and C. Mirodatos, Hydrogen production from ethanol steam reforming in a micro-channel reactor. *Int. J. Hydrogen Energy*, 2010, **35**, 1152-1159.
- [8] A. Carrero, J.A. Calles, and A.J. Vizcaíno, Effect of Mg and Ca addition on coke deposition over Cu–Ni/SiO<sub>2</sub> catalysts for ethanol steam reforming. *Chem. Eng. J.* 2010, **163**, 395-402.
- [9] S.I. Ito, and K. Tomishige, Steam reforming of ethanol over metal-oxide-promoted Pt/SiO<sub>2</sub> catalysts: Effects of strong metal-oxide interaction (SMOI). *Catal. Commun.* 2010, **12**, 157-160.
- [10] A.L. Alberton, M.M.V.M. Souza, and M. Schmal, Carbon formation and its influence on ethanol steam reforming over Ni/Al<sub>2</sub>O<sub>3</sub> catalysts. *Catal. Today*, 2007, **123**, 257-264.
- [11] J. Comas, F. Mariño, M. Laborde, and N. Amadeo, Bio-ethanol steam reforming on Ni/Al<sub>2</sub>O<sub>3</sub> catalyst. *Chem. Eng. J.* 2004, **98**, 61-68.
- [12] G.A. Deluga, J.R. Salge, L.D. Schmidt, and X.E. Verykios, Renewable hydrogen from ethanol by autothermal reforming. *Science*, 2004, **303**, 993-997.
- [13] F. Frusteri, and S. Freni, Bio-ethanol, a suitable fuel to produce hydrogen for a molten carbonate fuel cell. *J. Power Sources*, 2007, **173**, 200-209.
- [14] H. Idriss, M. Scott, J. Llorca, S.C. Chan, W. Chiu, P.Y. Sheng, A. Yee, M.A. Blackford, S. Pas, A.J. Hill, F.M. Alamgir, R. Rettew, C. Petersburg, S.D. Senanayake, and M.A. Barteau, A Phenomenological Study of the Metal–Oxide Interface: The Role of Catalysis in Hydrogen Production from Renewable Resources. *Chem. Sus. Chem.* 2008, **1**, 905-910.

- [15] A.E. Galetti, M.F. Gomez, L.A. Arrua, A.J. Marchi, and M.C. Abello, Study of CuCoZnAl oxide as catalyst for the hydrogen production from ethanol reforming. *Catal. Commun.* 2008, **9**, 1201-1208.
- [16] J.Y. Liu, C.C. Lee, C.H. Wang, C.T. Yeh, and C.B. Wang, Application of nickel–lanthanum composite oxide on the steam reforming of ethanol to produce hydrogen. *Int. J. Hydrogen Energy*, 2010, **35**, 4069-4075.
- [17] H. Muroyama, R. Nakase, T. Matsui, and K. Eguchi, Ethanol steam reforming over Ni-based spinel oxide. *Int. J. Hydrogen Energy*, 2010, **35**, 1575-1581.
- [18] M. Numata, R. Takahashi, I. Yamada, K. Nakanishi, and S. Sato, Sol–gel preparation of Ni/TiO<sub>2</sub> catalysts with bimodal pore structures. *Appl. Catal. A: Gen.*, 2010, **383**, 66-72.
- [19] R. Takahashi, S. Sato, S. Tomiyama, T. Ohashi, and N. Nakamura, Pore structure control in Ni/SiO<sub>2</sub> catalysts with both macropores and mesopores. *Micropor. Mesopor. Mat.* 2007, **98**, 107-114.
- [20] L. Zhao, K. Fang, D. Jiang, D. Li, and Y. Sun, Sol–gel derived Ni–Mo bimetallic carbide catalysts and their performance for CO hydrogenation. *Catal. Today*, 2010, **158**, 490-495.
- [21] K. Peng, L. Zhou, A. Hu, Y. Tang, and D. Li, Synthesis and magnetic properties of Ni–SiO<sub>2</sub> nanocomposites. *Mater. Chem. Phys.* 2008, **111**, 34-37.
- [22] K.H. Wu, and W.C. Huang, Effect of varying the acid to metal ion ratio R on the structural and magnetic properties of SiO<sub>2</sub>-doped Ni–Zn ferrite. *J. Solid State Chem.* 2004, **177**, 3052-3057.
- [23] J.B. Pang, K.Y. Qiu, and Y. Wei, Preparation of mesoporous silica materials with non-surfactant hydroxy-carboxylic acid compounds as templates via sol–gel process. *J. Non-Cryst. Solids*, 2011, **283**, 101-108.
- [24] R. Takahashi, S. Sato, T. Sodesawa, M. Kato, S. Takenaka, and S. Yoshida, Structural and catalytic properties of Ni/SiO<sub>2</sub> prepared by solution exchange of wet silica gel. *J. Catal.* 2001, **204**, 259-271.
- [25] S.K. Saraswat, and K.K. Pant, Synthesis of hydrogen and carbon nanotubes over copper promoted Ni/SiO<sub>2</sub> catalyst by thermocatalytic decomposition of methane. *J. Natural Gas Sci. Eng.*, 2013, **13**, 52-59.
- [26] N. Tang, L. Lü, W. Zhong, C. Au, and Y. Du, Synthesis and magnetic properties of carbon-coated Ni/SiO<sub>2</sub> core/shell nanocomposites. *Science in China Series G: Phys., Mech. Astro.*, 2009, **52**, 31-34.
- [27] D.W. Lee, S.K. Ihm, and K.H. Lee, Mesoporous silica framed by sphere-shaped silica nanoparticles. *Micropor. Mesopor. Mat.*, 2005, **83**, 262-268.
- [28] R. Takahashi, S. Sato, T. Sodesawa, M. Kawakita, and K. Ogura, High surface-area silica with controlled pore size prepared from nanocomposite of silica and citric Acid. *J. Phys. Chem. B*, 2000, **104**, 12184-12191.
- [29] C. Wu, and P.T. Williams, Hydrogen production from steam reforming of ethanol with nano-Ni/SiO<sub>2</sub> catalysts prepared at different Ni to citric acid ratios using a sol–gel method. *Appl. Catal. B: Environ.*, 2011, **102**, 251-259.

- [30] B.J. McBride, and S. Gordon, Computer program for calculation of complex chemical equilibrium compositions and applications II. Users manual and program description., NASA Lewis Research Centre, 1996.
- [31] R. Md Zin, A.B. Ross, M. Jones and V. Dupont, Hydrogen from ethanol reforming with aqueous fraction of pine pyrolysis oil with and without chemical looping. *Bioresour. Technol.*, 2015, **176**, 257-266.
- [32] R. Takahashi, S. Sato, T. Sodesawa, M. Suzuki, and N. Ichikuni, Ni/SiO<sub>2</sub> prepared by sol-gel process using citric acid. *Micropor. Mesopor. Mat.*, 2003, **66**, 197-208.
- [33] R. Takahashi, S. Sato, T. Sodesawa, M. Yoshida, and S. Tomiyama, Addition of zirconia in Ni/SiO<sub>2</sub> catalyst for improvement of steam resistance. *App. Cata. A: Gen.*, 2004, **273**, 211-215.
- [34] Sing, K. S. W. (1985), Reporting physisorption data for gas/solid systems with special reference to the determination of surface area and porosity (Recommendations 1984). *Pure and Applied Chemistry*.
- [35] M. Kong, J. M., Fei, S. Wang, W. Lu, and X. Zheng, Influence of supports on catalytic behavior of nickel catalysts in carbon dioxide reforming of toluene as a model compound of tar from biomass gasification. *Bioresour. Technol.*, 2011, **102**, 2004-2008.
- [36] K.O. Christensen, D. Chen, R. Lødeng, and A. Holmen, Effect of supports and Ni crystal size on carbon formation and sintering during steam methane reforming. *Appl. Catal. A: Gen.*, 2006, **314**, 9-22.

Table 1 Surface properties of investigated catalysts prepared at different conditions

Catalyst	Conditions <sup>a</sup> A-B-C	pH <sup>b</sup>	BET (m <sup>2</sup> g <sup>-1</sup> )	BJH pore Volume (cm <sup>3</sup> g <sup>-1</sup> )	BJH pore diameter (nm)
Ni/SiO <sub>2</sub> -1	HNO <sub>3</sub> -0.20-Air	1.00	829	0.665	3.8
Ni/SiO <sub>2</sub> -2	HNO <sub>3</sub> -0.04-Air	1.10	737	0.698	3.8
Ni/SiO <sub>2</sub> -3	NH <sub>4</sub> OH-0.04-Air	1.50	707	0.640	3.8
Ni/SiO <sub>2</sub> -4	NH <sub>4</sub> OH-0.20-Air	2.08	605	0.575	3.2-5.0
Ni/SiO <sub>2</sub> -5	HNO <sub>3</sub> -0.20-N <sub>2</sub>	1.00	810	0.581	3.8
Ni/SiO <sub>2</sub> -6	HNO <sub>3</sub> -0.04-N <sub>2</sub>	1.10	807	0.590	3.8
Ni/SiO <sub>2</sub> -7	NH <sub>4</sub> OH-0.04-N <sub>2</sub>	1.50	797	0.619	3.8
Ni/SiO <sub>2</sub> -8	NH <sub>4</sub> OH-0.20-N <sub>2</sub>	2.08	545	0.309	3.8-5.0

<sup>a</sup> A-agent; B-agent/TEOS molar ratio; C-calcination atmosphere

<sup>b</sup> pH value was determined after addition of agent (HNO<sub>3</sub> or NH<sub>4</sub>OH)

Table 2 Mass balance and gas compositions for ethanol steam reforming with the prepared catalysts, carrier gas is included in the gas composition. Equilibrium H<sub>2</sub> yield was 23.2 wt% of etOH.

Reducing atmosphere		Air				N <sub>2</sub>			
Catalyst	Ni/SiO <sub>2-x</sub> . x=1-8	1	2	3	4	5	6	7	8
Mass balance (wt.% of feed)									
	Measured gas yield	57.5	56.7	58.9	58.2	65.3	66.4	62.2	63.0
	Measured liquid yield	35.9	35.5	36.1	34.8	32.3	31.3	35.4	33.6
	Calculated balance closure	6.5	7.6	4.8	6.8	2.3	2.2	2.2	3.3
	Coke formation (wt.%)	1.8	2.9	3.8	4.0	1.5	1.6	2.8	2.3
Hydrogen Yield									
	(% Eq. value)	66.5	66.6	68.4	66.7	70.7	71.6	72.0	69.2
Gas Composition									
(Vol.%)									
	CO	4.2	4.3	4.8	4.5	5.3	5.4	4.5	5.4
	H <sub>2</sub>	24.3	24.6	26.3	25.6	25.1	25.0	23.9	26.3
	N <sub>2</sub>	63.8	63.4	60.8	61.7	61.3	61.4	64.2	59.7
	CO <sub>2</sub>	6.3	6.2	6.6	6.7	6.5	6.5	6.0	6.8
	CH <sub>4</sub>	1.4	1.5	1.6	1.5	1.8	1.9	1.4	1.8
	H <sub>2</sub> purity in gas	67.1	67.2	66.9	66.8	64.9	64.4	66.8	65.3
(N <sub>2</sub> free, Vol.%)									

Table 3 Experimental selectivity (%) to gas products and calculated equilibrium selectivity

Reducing atmosphere Catalyst Ni/SiO <sub>2-x</sub> . x=1-8	Air				N <sub>2</sub>				Calc. Equil.
	1	2	3	4	5	6	7	8	
C-products <sup>a</sup>									
Sel CO	35.3	35.8	36.9	35.4	39.0	39.1	37.8	38.6	25.6
Sel CO <sub>2</sub>	52.9	51.7	50.8	52.8	47.8	47.1	50.4	48.6	72.1
Sel <sub>C</sub> CH <sub>4</sub>	11.8	12.5	12.3	11.8	13.2	13.8	11.8	12.9	2.3
H-products <sup>b</sup>									
Sel <sub>H</sub> CH <sub>4</sub>	10.3	10.9	10.8	10.5	12.5	13.2	10.5	12.0	1.7
Sel H <sub>2</sub>	89.7	89.1	89.2	89.5	87.5	86.8	89.5	88.0	98.2

<sup>a</sup> e.g. Sel CO = 100 × Vol.% CO / Vol.%(CO+CO<sub>2</sub>+CH<sub>4</sub>);

<sup>b</sup> Sel H<sub>2</sub> = 100 × Vol.% H<sub>2</sub> / Vol.%(H<sub>2</sub>+2CH<sub>4</sub>); Sel<sub>H</sub> CH<sub>4</sub> = 100 × 2 × vol% CH<sub>4</sub> / vol%(H<sub>2</sub>+2CH<sub>4</sub>)

## FIGURE CAPTIONS

Figure 1 H<sub>2</sub> yield weight percent of ethanol feed from the EtOH/H<sub>2</sub>O/N<sub>2</sub> equilibrium system at various reforming temperatures and steam/carbon ratios (equilibrium study). Other experimental conditions: preheating temperature-190 °C, carrier gas (N<sub>2</sub>) flow rate-80 ml min<sup>-1</sup>; total raw material (ethanol and water) flow: 3.44 g h<sup>-1</sup>

Figure 2 XRD analysis for selected prepared catalysts; (a) Ni/SiO<sub>2</sub>-4, (b) Ni/SiO<sub>2</sub>-8, (c) Ni/SiO<sub>2</sub>-1, (d) Ni/SiO<sub>2</sub>-5

Figure 3 N<sub>2</sub> adsorption/desorption isotherms of the selected fresh catalysts

Figure 4 TEM analysis of the prepared fresh catalysts

Figure 5 TGA-TPO and DTG-TPO results of the selected reacted catalyst

Figure 6 SEM and TEM results of reacted Ni/SiO<sub>2</sub> catalyst; (a) (b) typical SEM results, (c) (d) typical TEM results

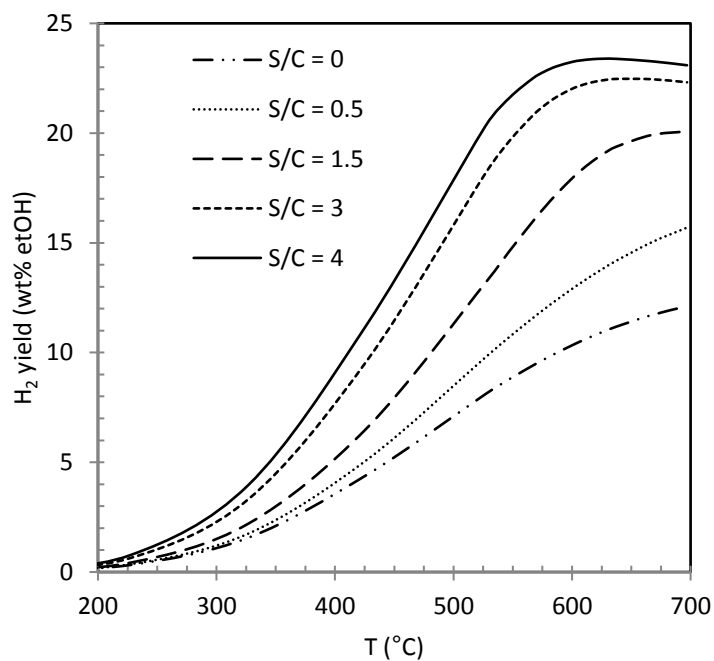


Figure 1 H<sub>2</sub> yield weight percent of ethanol feed from the EtOH/H<sub>2</sub>O/N<sub>2</sub> equilibrium system at various reforming temperatures and steam/carbon ratios (equilibrium study). Other experimental conditions: preheating temperature-190 °C, carrier gas (N<sub>2</sub>) flow rate-80 ml min<sup>-1</sup>; total raw material (ethanol and water) flow: 3.44 g h<sup>-1</sup>

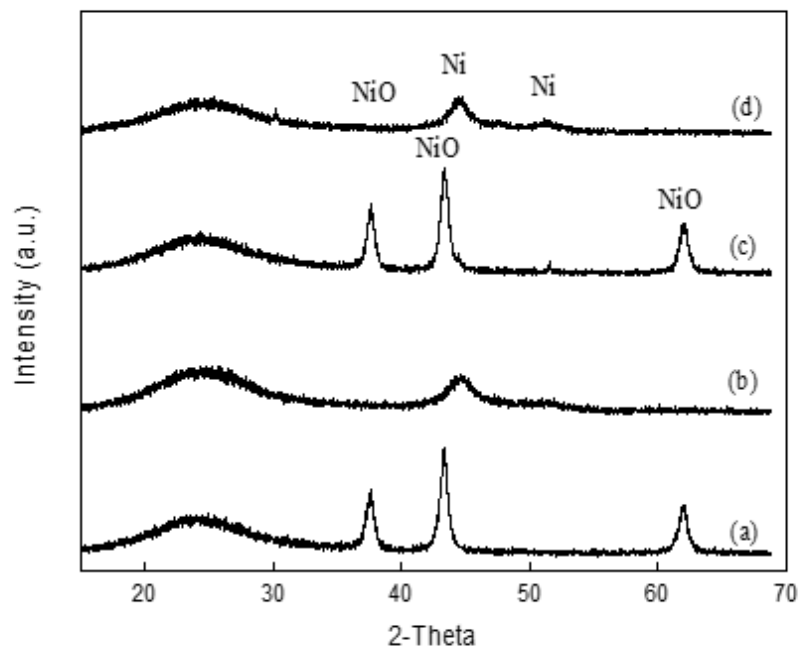


Figure 2 XRD analysis for selected prepared catalysts; (a) Ni/SiO<sub>2</sub>-4, (b) Ni/SiO<sub>2</sub>-8, (c) Ni/SiO<sub>2</sub>-1, (d) Ni/SiO<sub>2</sub>-5

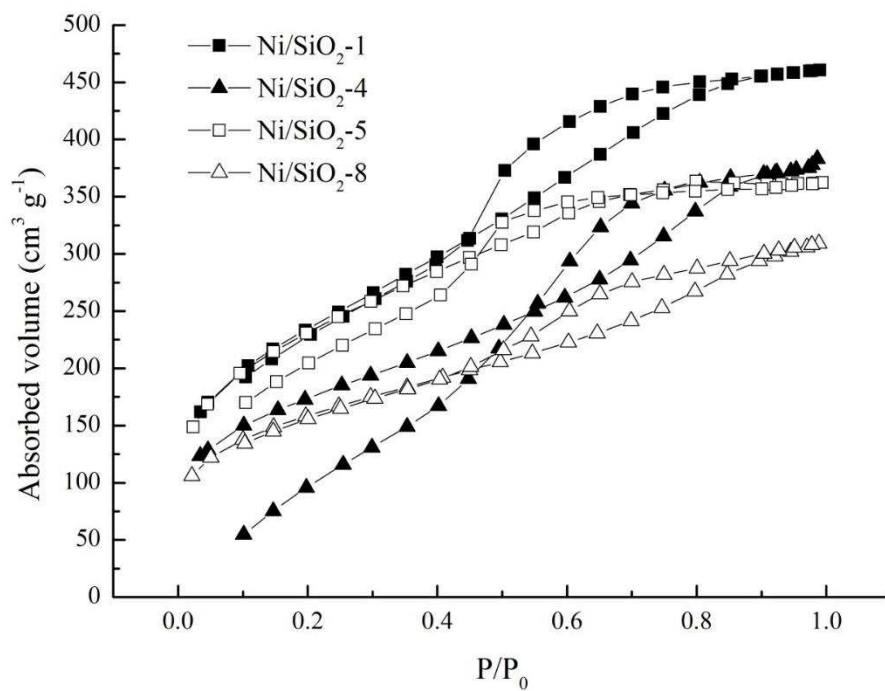
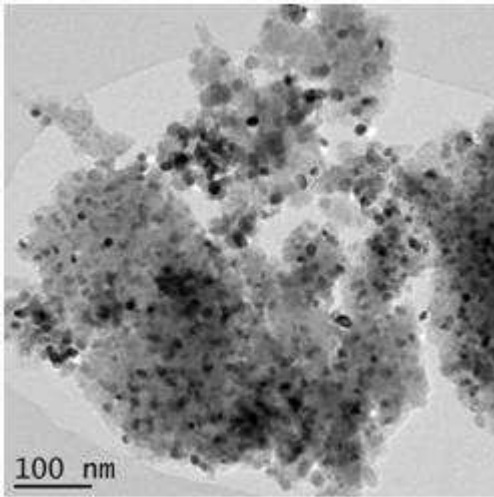
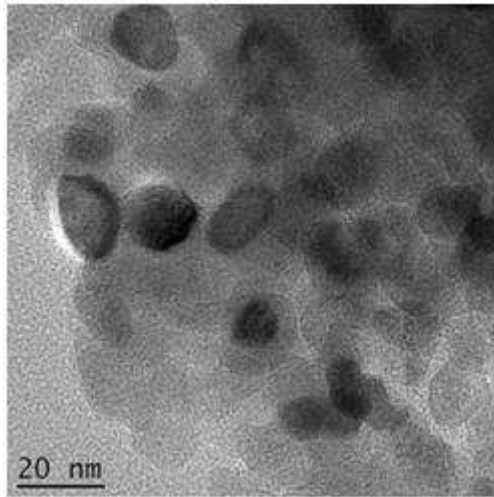


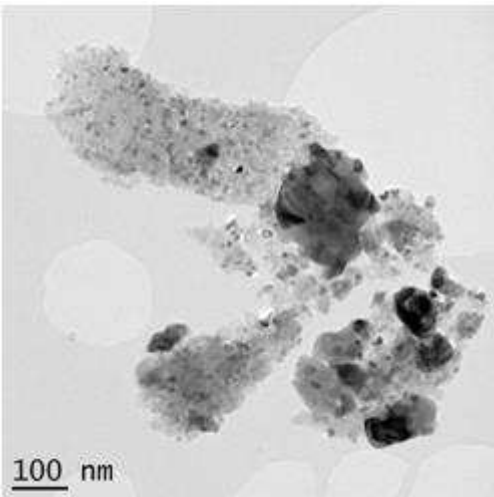
Figure 3 N<sub>2</sub> adsorption/desorption isotherms of the selected fresh catalysts



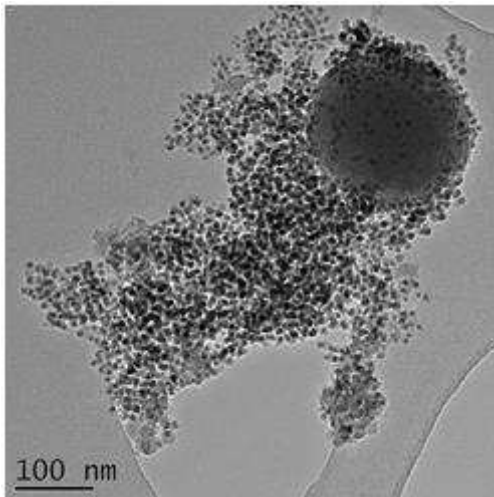
Fresh Ni/SiO<sub>2</sub>-(1-3)



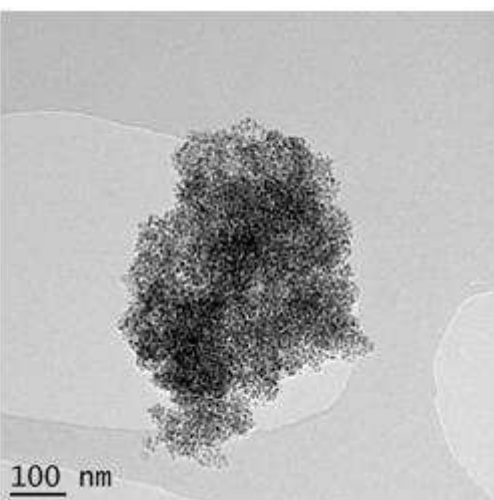
Fresh Ni/SiO<sub>2</sub>-(1-3)



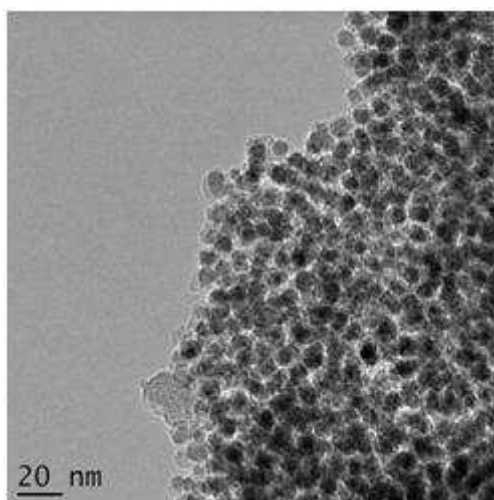
Fresh Ni/SiO<sub>2</sub>-4



Fresh Ni/SiO<sub>2</sub>-8



Fresh Ni/SiO<sub>2</sub>-(5-7)



Fresh Ni/SiO<sub>2</sub>-(5-7)

Figure 4 TEM analysis of the prepared fresh catalysts

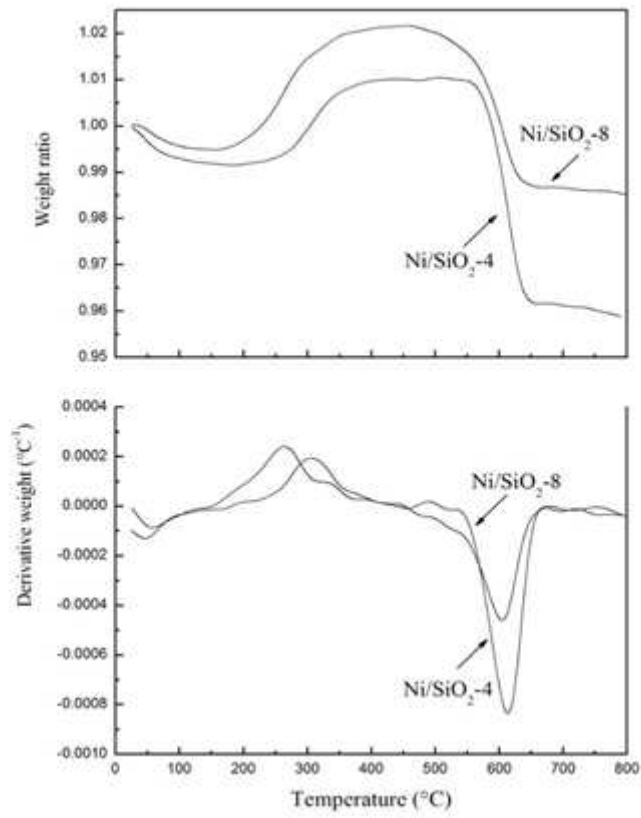
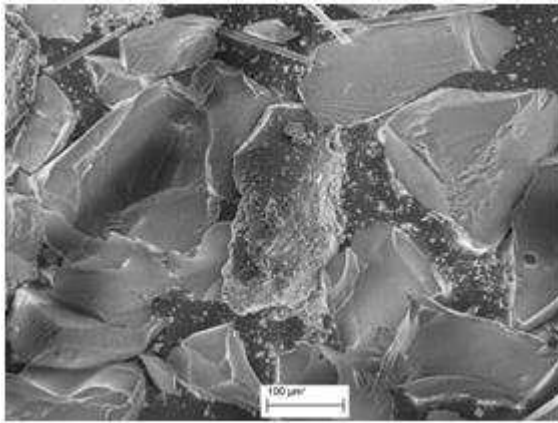
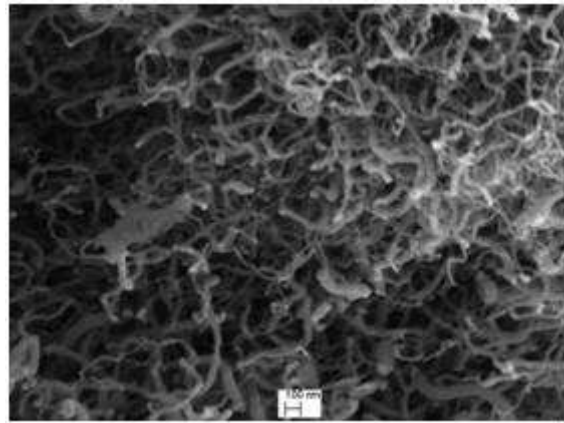


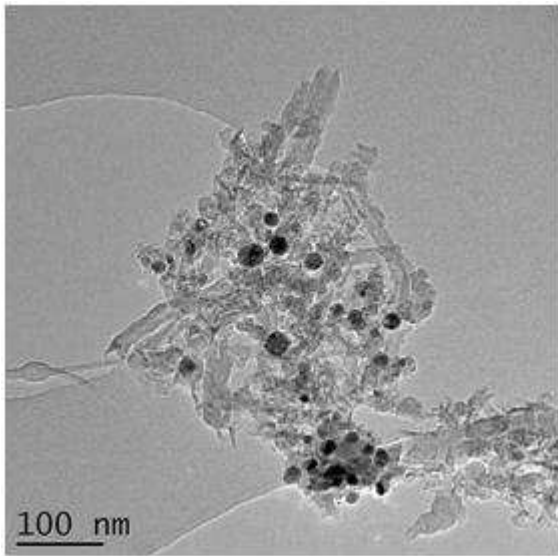
Figure 5 TGA-TPO and DTG-TPO results of the selected reacted catalyst



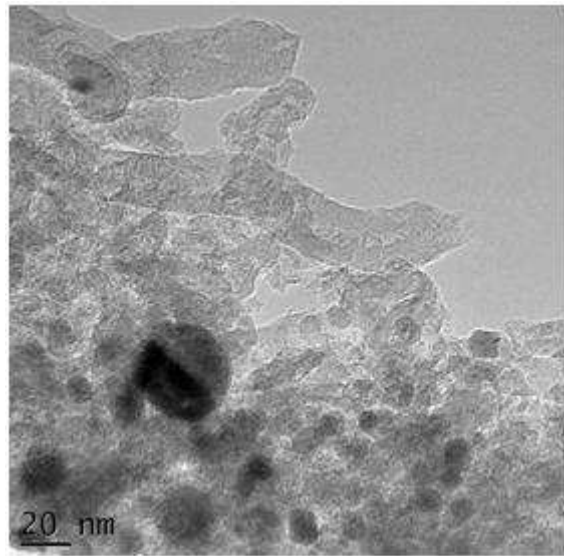
(a)



(b)



(c)



(d)

Figure 6 SEM and TEM results of reacted Ni/SiO<sub>2</sub> catalyst; (a) (b) typical SEM results, (c) (d) typical TEM results